EXPLORATORY SYNTHESIS AND REDOX BEHAVIOR OF THE F-BLOCK

by

Megan Whitefoot

A Thesis

Submitted to the Faculty of Purdue University

In Partial Fulfillment of the Requirements for the degree of

Master of Science

Department of Chemistry

West Lafayette, Indiana

August 2021

THE PURDUE UNIVERSITY GRADUATE SCHOOL

STATEMENT OF COMMITTEE APPROVAL

Dr. Suzanne Bart Chair

Department of Chemistry

Dr. Tong Ren

Department of Chemistry

Dr. Corey Thompson

Department of Chemistry

Approved by:

Dr. Christine Hrycyna

Dedicated to Joseph Michael Sperling, Boba and Ludo

ACKNOWLEDGMENTS

I am so thankful to have had the best boss in the field. Dr. Suzanne Bart has been my biggest supporter for the last two years. She has helped me grow so much and learn to be confident in myself. I am beyond grateful for all the opportunities she has given me. She has shown me how much potential I have regardless of the career I choose. Dr. Bart saw me in my most vulnerable states and was never judgmental. I feel like I do not deserve the amount of kindness she has shown me. Through every difficult decision I must make, she stands behind me cheering on. I have never met anyone as intelligent and as caring as her. She is going to go so far in this field because of how much she supports her students. Although I am leaving way too soon and unexpectedly, I will never forget the experiences and lessons I learned in the Bart group. Being here was so much more than just doing science, it was obtaining valuable life lessons and gaining long lasting friendships. Thank you, Suzanne, and thank you Austin and Finley for being my best buddies. I would also like to thank my group members for helping me so much in lab, especially Dr. Jerod Kieser and Madeleine Uible. I would also like to thank Miranda Weigand and Kadidia Samassekou for being amazing friends through my entire graduate school journey. Dr. Joseph Sperling, you already know how thankful I am for you and your support, no words can describe it. Lastly, I would like to thank my family for always believing in me through all my academic journeys and life choices. I know my choice to leave Purdue was unexpected, but I am coming home to heal and grow into the best version of myself. I loved this experience at Purdue with all of my heart and I can't wait to see everyone again very soon! Boiler up! Hammer down! May the force be with you all! Stay spooky.

TABLE OF CONTENTS

LIST OF TABLES

LIST OF FIGURES

ABSTRACT

The interest in understanding the *f*-block elements has been increasing because of the large applications of these elements across all fields of science and technology. The lanthanides are used in various technologies like car batteries and phone screens. The actinides are the basis of current nuclear fuel processes. The *f* -block has many interesting properties and has been proven to be fruitful in inorganic chemistry. Neodymium is redox inactive and was studied with a redox active ligand pyridine diimine to see if multielectron chemistry was viable. The neodymium chemistry is still in the preliminary stages of research, but there is possibility of fruitful reactivity. Recently neptunium chemistry was introduced to the Bart lab to study its rich redox chemistry. Neptunium's fundamental properties have been investigated for the last 80 years with new bonding properties and behavior still being discovered today. Studies of neptunium began with investigating the trivalent oxidation state. Synthesis of new low valent trans-uranic starting materials is important because the fundamental chemistry of these trivalent compounds is not well studied. By creating Neptunium materials that are analogous to known uranium and lanthanide starting materials, *f*-block chemists will be able to apply their previously studied syntheses to a new element.

CHAPTER 1. NEPTUNIUM NOVEL STARTING MATERIALS

1.1 Abstract

1.2 Introduction

The lack of knowledge of the coordination chemistry of trans-uranium elements when compared to uranium and thorium is due in part to the scarcity of these person-made elements and the need for specialized radiological facilities to accommodate for the hazards of these materials. [1.1] In addition to the dangers of its radiotoxicity, neptunium metal is difficult to make and access to it is restricted.[1.2] Modern ^{237}Np research is involves studying the redox chemistry of the element in aqueous and nonaqueous media to aid in spent nuclear fuel separations. [1.3] Like plutonium, neptunium accesses oxidation states ranging from +2 to +7, which makes it more versatile compared to the +3 lanthanides and later actinides. By studying the chemical behavior of these highly radioactive nuclei in varying oxidation states, new and safer methods for spent nuclear fuel separations can be developed and optimized. Typically, lanthanides are used for modeling of trans-uranium elements, thus trivalent actinides specifically are of interest to investigate if there are significant differences between the elements for separations chemistry.

Solvated actinide trihalides have been known to be a useful class of actinide materials that traditionally are made from the elemental metal and elemental dihalide[1.4]. For example, $UI_3(THF)_4$ (THF = tetrahydrofuran) was synthesized by Clark, Sattelberger, and coworkers in 1989 using uranium metal and elemental I_2, which is still the method used to make this material today.[1.5] Evolution of this material to $UI_3(dioxane)_{1.5}$ is performed in an analogous manner, substituting dioxane for the THF.[1.6] $UBr_3(THF)_4$ was also synthesized in this way, except with

elemental bromine, in 1994 by Zwick and coworkers.[1.7] These syntheses are useful for uranium materials since the metal is abundant.

In the case of neptunium, the elemental metal is hard to obtain and is not available in large quantities. [1.3] With this problem in mind, we set out to establish a convenient entry into trivalent neptunium starting materials beginning from neptunia (NpO_2) which is more readily available than the metal. Inspired by the previously synthesized trivalent solvate, $NpCl_3(py)_4$ (py= pyridine), completing the trivalent neptunium halide series using improved synthetic methods were desired.[1.8] Recently reported, the analogous uranium trivalent solvated halides ($UBr_3(THF)_4$ and $UI_3(THF)_4$) were made similarly using the synthetic methods we report here with neptunium by Daly and coworkers.[1.9]

Herein we report the synthesis and characterization of two Np (III) non-aqueous solvated halides, $NpI_3(THF)_4$ (**1**) and $NpBr_3(THF)_4$ (**2**) and note the differences between the two structures and their uranium analogs versus previous synthetic methods used to make these compounds. All compounds were fully characterized by single crystal X-ray crystallography, ^{1}H NMR spectroscopy, and electronic absorption spectroscopy.

1.3 Experimental details

General Considerations. Caution! ^{237}Np represents a health risk due to its α and γ emission and its decay to the short-lived ^{233}Pa isotope ($t_{1/2}$= 27.0 days), which is a strong β and γ emitter. All studies with Np were conducted in a laboratory equipped for radioactive materials. All air- and moisture-sensitive manipulations were performed using standard Schlenk techniques or in an MBraun inert atmosphere drybox with an atmosphere of argon. The MBraun drybox was equipped with a cold well designed for freezing samples in liquid nitrogen as well as one −35 °C freezer for cooling samples and crystallizations. Solvents for sensitive manipulations were dried

and deoxygenated using literature procedures with a Seca solvent purification system. THF-d8 and DCM-d2 were purchased from Cambridge Isotope Laboratories and were used without further purification. $CDCl_3$ was purchased from Cambridge Isotope Laboratories, dried with molecular sieves and sodium, and degassed by three freeze−pump−thaw cycles. Trimethylsilyl chloride (TMS-Cl) and trimethylsilyl bromide (TMS-Br) were purchased from Sigma-Aldrich and were stirred over CaH_2 and distilled before use. Trimethylsilyl iodide (TMS-I) was purchased from Sigma-Aldrich and used as received. HCl 37% was purchased from Honeywell and used without further purification. 48-51% HF solution in water was purchased from Acros Organics and used without further purification. Potassium graphite (KC_8) were prepared according to literature procedures. ^{1}H NMR spectra were recorded on a Varian Inova 300 or Bruker AV-III-HD-400 spectrometer operating at 299.99 and 400.13 MHz, respectively. All chemical shifts were reported relative to the peak for $SiMe_4$ using 1H (residual) chemical shifts of the solvent as a secondary standard. The spectra for paramagnetic molecules were obtained using an acquisition time of 0.5 s; thus, the peak widths reported have an error of ±2 Hz. For paramagnetic molecules, the ^{1}H NMR data are reported with the chemical shift, followed by the peak width at half height in hertz, the integration value, and where possible, the peak assignment. Electronic absorption measurements were recorded at 294 K in THF in sealed 1 cm short path quartz cuvettes with data collection being performed on an Agilent Cary 6000i UV-Vis-NIR Spectrophotometer.

Preparation of $NpCl_4(DME)_2$. In the glovebox, solid NpO_2 (55.5 mg, 0.21 mmol) was weighed into a pre-weighed 20 mL scintillation vial. This vial was removed from the glovebox and placed onto a heating mantle with sand. 4 mL of 8 M HCl was added to the NpO_2 powder resulting in a partially dissolved brown-green solution. In order to fully dissolve the oxide, 10

microliters of HF were added. The solution was then heated to 80 °C and agitated until the solution was clear. Since we start from NpO_2 and only have the Np in aqueous media for about 30 minutes, we do not see oxidation impurities such as the V oxidation state therefor no hydroxyl amine is needed. The solution was then dried to a purple-brown powder with heat (80 °C) and argon. The vial was then covered with a kim wipe and secured with a rubber band and placed into the antechamber for 48 hours. The resulting deep pink powder was suspended in DME and heated at 50 °C for an hour. TMS-Cl was added in excess (5 mL) until the solution turned clear orange. The solution was then stirred and heated at 50 °C for 4 hours. The heat was turned off and the solution stirred overnight. The pink solution was then vacuumed down to a pink powder. The powder was washed with cold ether. Volatiles were removed in vacuo and the resulting solid was washed with pentane to afford a pink powder obtained and afforded to $NpCl_4(DME)_2$ in good yield (111.0 mg, 96.3%).

Preparation of $Np_2Cl_8(DME)_2$. $NpCl_4(DME)_2$ was dissolved in 1 mL $CDCl_3$ then added to a NMR tube. The tube was left at room temperature for 24 hours resulting in pink crystals afforded to be $Np_2Cl_8(DME)_2$.

Preparation of $NpCl_6(NH_3OH)_2$. $NpCl_4(DME)_2$ was synthesized using hydroxyl amine HCl to ensure oxidation state purity. In result this salt complex was formed when dissolved in THF and grown overnight at –35 °C. The colorless salt crystals were determined to be $[NpCl_6]^{2-}$ $[(NH_3OH)]^{2+}$

NMR Preparation of $NpI_3(THF)_4$. $NpCl_4(DME)_2$ was added to an NMR tube and dissolved in $CDCl_3$. TMS-I was added in excess resulting in an immediate color change of light pink to red. The red solution then precipitated a black solid in the tube. The red solution was removed, and the black solution was suspended in DME resulting in a green solution. This

solution was pumped down to a residue and was set to crystallize in a vapor diffusion of pentane into DME. This crystallization was unsuccessful, so the solution was pumped down into a powder. This powder was dissolved in THF resulting in a gold solution and set to crystallize in a vapor diffusion of pentane and THF. X-ray quality gold crystals were grown overnight in a good yield. These gold crystals were determined to be $NpI_3(THF)_4$. This product is not soluble in CDCl3 so the ^1H NMR spectrum shows biproduct TMS-Cl at 0.48 ppm and excess TMS-I at 0.84 ppm.

Preparation of $NpI_3(THF)_4$. Solid $NpCl_4(DME)_2$ (14.8 mg, 0.026 mol) was weighed into a pre-weighed 20 mL scintillation vial and a Teflon stir bar was added. The pink powder was dissolved and stirred in 2 mL of THF for five minutes. Me_3SiI (50.6 mg or 36 μL, 0.051 mmol, 8 equiv. with respect to Np) was added with a micro-syringe to the dissolved $NpCl_4$ at room temperature which caused a color change from light pink to a red-yellow solution. This solution was stirred for an hour resulting in a golden-brown solution. To remove excess I_2, the solution was pumped down to a brown residue. This residue was washed with pentane until the washes were colorless. The orange-brown sticky solid was dried in vacuo for an hour. This powder was washed again with ether (3 mL) to afford a golden powder (yield: 18 mg, 74.5%). Gold crystals were grown from a vapor diffusion of pentane into the THF solution at –35C.

Alternative preparation of $NpI_3(THF)_4$. Solid $NpCl_4(DME)_2$ (21.0 mg, 0.038 mmol) was weighed into a pre-weighed scintillation vial and a Teflon stir bar was added. The pink powder was dissolved in 1 mL THF and stirred for five minutes. Solid KC_8 (5.07 mg, 1 eq) was slowly added to the solution creating a dark green slurry. After stirring for an hour, the solution was filtered through glass filter paper resulting in a light green solution of $NpCl_3(THF)_X$. TMS-I (13.7 μL, 3 eq) was syringed into the $NpCl_3(THF)_X$ solution causing a color changed from green

to gold. The solution was pumped down to a residue afforded to be $NpI_3(THF)_4$ (16.1 mg, 0.018 mmol 47% yield). X-ray quality crystals were grown from a vapor diffusion of pentane into a concentrated THF solution at –35 °C and matched the unit cell of the previously reported $NpI_3(THF)_4$.

Preparation of $[H(THF)_2]^+[NpBr_5THF]^-$. Solid $NpCl_4(DME)_2$ (9.1 mg) was weighed into a pre weighed scintillation vial and a Teflon stir bar was added. The powder was dissolved in THF and (10.20 μL, 4 eq) of TMS-Br x HBr was added. After stirring for one hour, the solution was pumped down and washed with pentane. X-ray quality crystals were grown from a vapor diffusion of pentane into THF at –35 °C determined to be$[H(THF)_2]^+[NpBr_5THF]^-$.

Preparation of $NpBr_3(THF)_4$. Solid $NpCl_4(DME)_2$ (10.0 mg, 0.018 mol) was weighed into a pre-weighed scintillation vial and a Teflon stir bar was added. The pink powder was dissolved in 1 mL THF and stirred for five minutes. Solid KC_8 (5.3mg, 1.5 eq) was slowly added to the solution creating a dark green slurry. After stirring for an hour, the solution was filtered through glass filter paper resulting in a light green solution of $NpCl_3(THF)_4$. TMS-Br (13.8 μL, 4 eq) was syringed into the $NpCl_3(THF)_4$ solution causing a color changed from green to yellow. The solution was pumped down to a residue afforded to be $NpBr_3(THF)_4$ (7.4 mg, 0.01 mmol 54% yield), . X-ray quality crystals were grown from a vapor diffusion of pentane into a concentrated THF solution at –35C.

1.4 Results and Discussion

Our experiments started with optimizing the synthesis of $NpCl_4(DME)_2$ the most common non-aqueous Np (IV) starting material previously reported by the Gaunt lab.[1.10]The optimized synthesis provides a 96.3% yield of pink crystalline $NpCl_4(DME)_2$. Complex 1 was fully characterized using single crystal X-ray diffraction (**Figure 1.1**) and ^1H NMR spectroscopy

(**Figure 1.2**). While attempting to crystallize this complex, a dimerized version was form resulting in $Np_2Cl_8(DME)_2$ (**Figure 1.3**). In addition, $NpCl_6(NH_3OH)_2$ was crystallized during the first syntheses when hydroxyl amine was used for oxidation state purity and dissolved in dioxane (**Figure 1.4**). This structure is what caused the removal of hydroxyl amine from the synthesis.

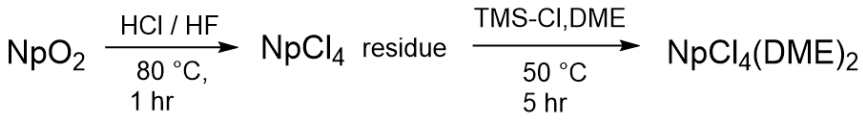

Figure 1.1 Synthesis of $NpCl_4(DME)_2$.

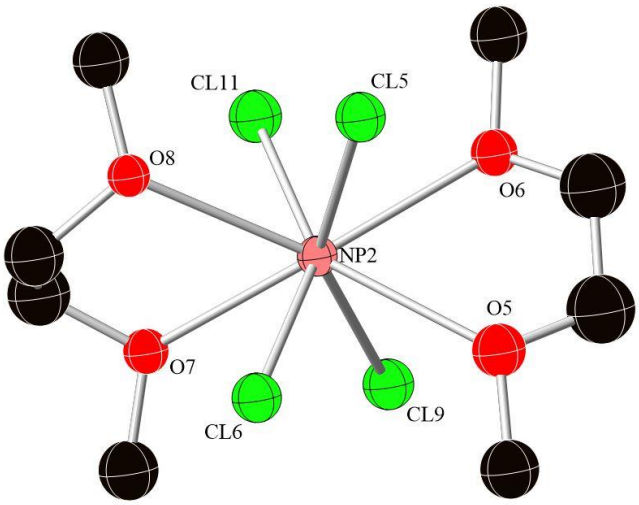

Figure 1.2. Thermal ellipsoid plot (at the 50% probability level) of the solid-state structure of $NpCl_4(DME)_2$ (1). Hydrogen atoms are omitted for clarity.

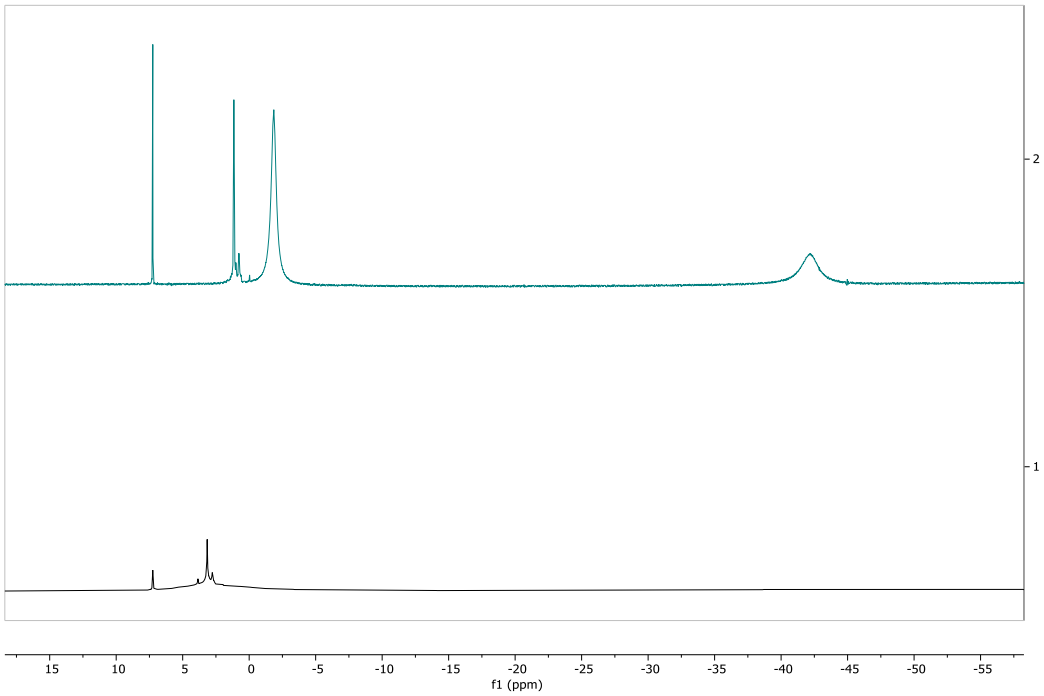

Figure 1.3. ^{1}H NMR spectrum of $NpCl_4(DME)_2$ in $CDCl_3$ (top) and DCM d2 (bottom). In CDCl3 the two coordinated DME broad peaks are assigned at -1.85 ppm and -42.1 ppm. In DCM d2 the two coordinated DME broad peaks are assigned at -1.13 ppm and -38.2 ppm.

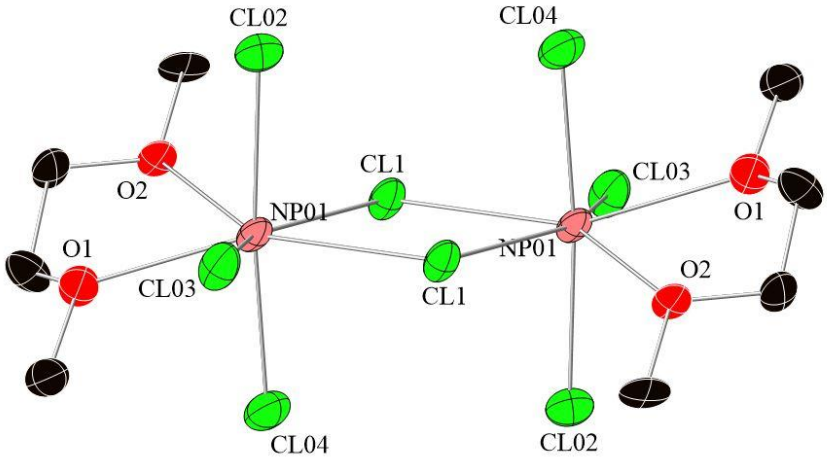

Figure 1.4 Thermal ellipsoid plot (at the 50% probability level) of the solid-state structure of $Np_2Cl_8(DME)_2$ (1). Hydrogen atoms are omitted for clarity.

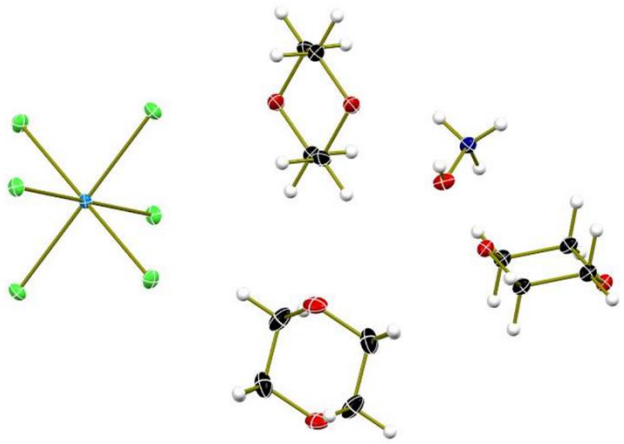

Figure 1.5 Thermal ellipsoid plot (at the 50% probability level) of the solid-state structure of $[NH_3OH]_2[NpCl_6]$•3dioxane (1). Hydrogen atoms are omitted for clarity.

With this starting material in high yield and purity, the investigation of Np (III) solvated halides commenced by using TMS-X (TMS= trimethyl silane X= I, Br) to exchange the chlorides from the $NpCl_4(DME)_2$.

The bond lengths in the previously reported $UI_3(THF)_4$ structure is used to compare to its neptunium analog (1) (Table 1). The NpI3(THF)4 crystallized in the space group $P2_1/c$ which is analogous to the uranium adduct. Both the uranium and neptunium structures are isomorphous and have a pentagonal bipyramid geometry with axial iodides. The Np-I bond lengths range from 3.0782(5) Å to 3.1462(6) Å and the U-I bond lengths previously reported range from 3.103(2) Å to 3.167(2) Å (**Table 1**).

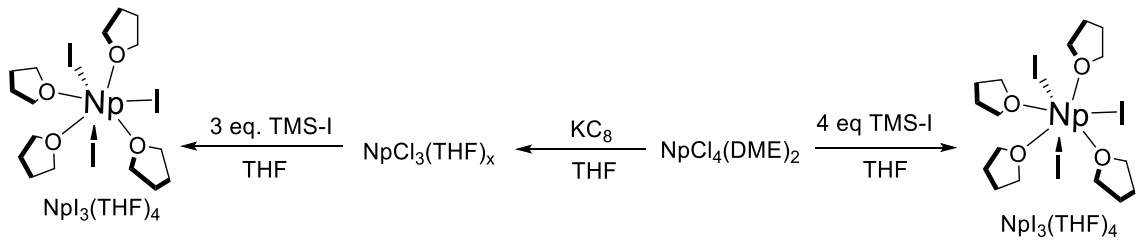

Figure 1.6 Synthesis of $NpI_3(THF)_4$.

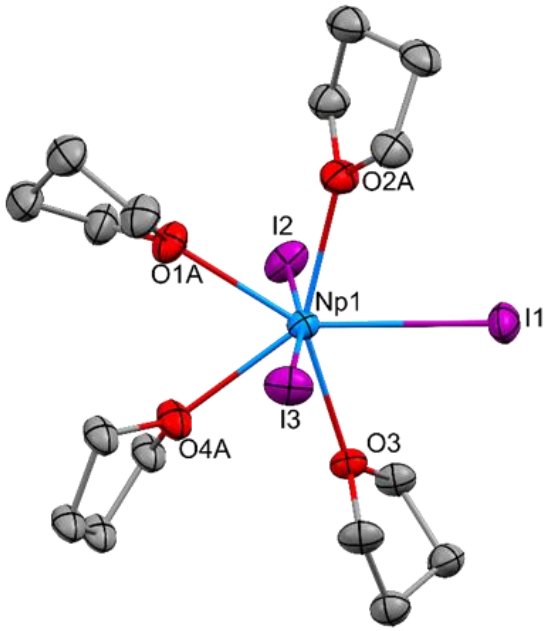

Figure 1.7 Thermal ellipsoid plot (at the 50% probability level) of the solid-state structure of $NpI_3(THF)_4$. Hydrogen atoms are omitted for clarity.

Table 1.1.1 Np–I, Np–THF, U-I and U-THF distances (in Å) for $NpI_3(THF)_4$ and $UI_3(THF)_4$.[1.5]

Bond	$NpI_3(THF)_4$	$UI_3(THF)_4$ [1.5]
M-I_{eq}	3.0782(5)	3.103 (2)
M-I_{eq}	3.0971(5)	3.119 (2)
M-I_{ax}	3.1462(6)	3.167(2)
M-O	2.471(4)	2.48(1)
M-O	2.494(4)	2.51(1)
M-O	2.504(4)	2.54(1)
M-O	2.541(5)	2.56(1)

Using the same reaction conditions as figure 1.8, $UBr_3(THF)_4$ was obtained. If there is excess HBr present in the TMS-Br, a $NpBr_5(THF)^-$ adduct if formed (figure 1.9). Both the uranium and neptunium structures were isomorphous and were comprised of a trivalent metal center in a pentagonal bipyramid geometry with axial bromides. The Np-Br bond lengths range from 2.8630 (10) Å to 2.8990 (10) Å and the U-Br bond lengths range from 2.8844(4) Å to 2.9138(4) Å.

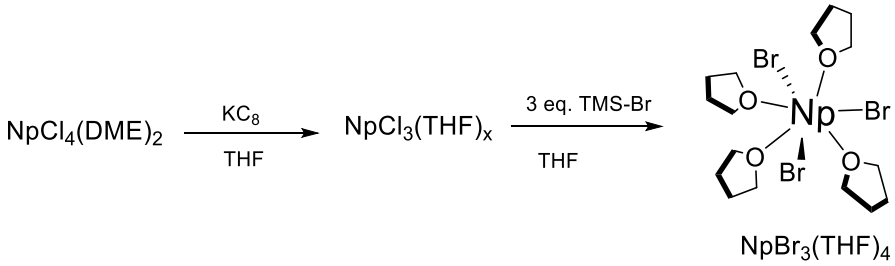

Figure 1.8 Synthesis of $NpBr_3(THF)_4$.

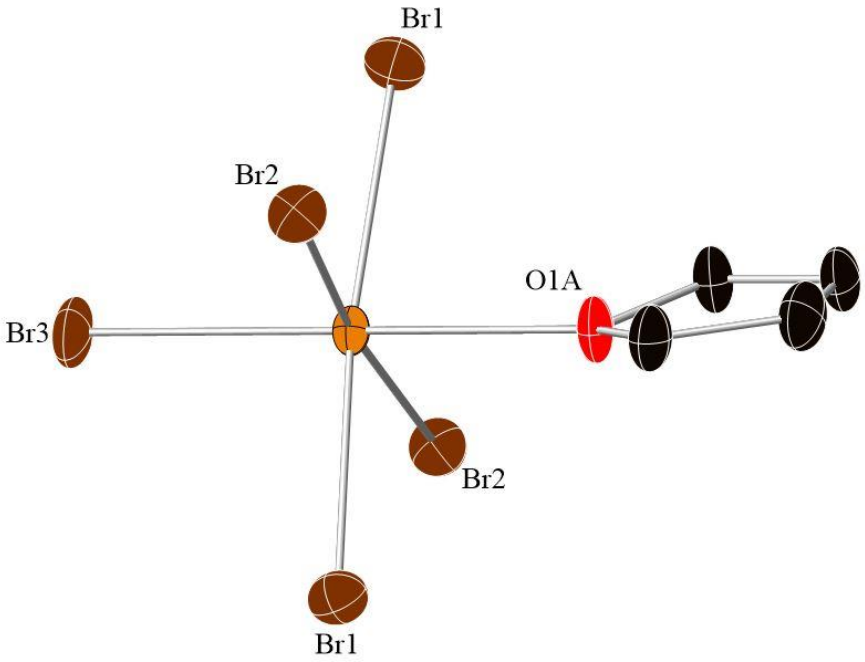

Figure 1.9 Thermal ellipsoid plot (at the 50% probability level) of the solid-state structure of $[NpBr_5THF]^-$. Hydrogen atoms are omitted for clarity.

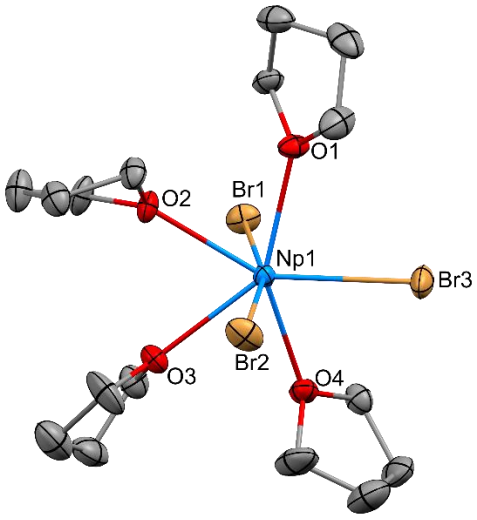

Figure 1.10 Thermal ellipsoid plot (at the 50% probability level) of the solid-state structure of $NpBr_3(THF)_4$. Hydrogen atoms are omitted for clarity.

Table 1.2 Np–Br, Np–THF, U-Br and U-THF distances (in Å) for $NpBr_3(THF)_4$ and $UBr_3(THF)_4$.

Bond	$NpBr_3(THF)_4$	$UBr_3(THF)_4$
M-Br $_{ax}$	2.8630(10)	2.8844(4)
M-Br $_{ax}$	2.8823(11)	2.9055(4)
M-Br $_{eq}$	2.8990(10)	2.9138(4)
M-O	2.501(5)	2.512(2)
M-O	2.504(5)	2.514(2)
M-O	2.531(5)	2.535(2)
M-O	2.562(5)	2.570(2)

When comparing $NpI_3(THF)_4$ to $NpBr_3(THF)_4$, both structures exhibit a distorted pentagonal bipyramidal geometry. In $NpBr_3(THF)_4$, the bromide is much more bent away from the pentagonal plane, 165.22(3)°, than the triiodide structure, 170.908(16)°. This is due to the size of the iodide, which prefers to be further away from the axial iodides.[1.12] The Np-halide

bond lengths in $NpI_3(THF)_4$ range from 3.0782(5) Å to 3.1462(6) Å and from 2.8630(10) Å to 2.8990(10) Å in $NpBr_3(THF)_4$. The bromide bond lengths are shorter than the iodide bonds due to the smaller size of the halide.

$NpI_3(THF)_4$ and $NpBr_3(THF)_4$ were studied by electronic absorption spectroscopy in the visible and near-IR regions (give nm) to further confirm the oxidation state of the metal. Compounds **1, 2**, and $NpCl_3(THF)_X$ (for reference) were dissolved in THF, and the solution spectra were taken in quartz screw-capped cuvettes. The spectra for both compounds share similar weak f-f transitions in the near IR region of 800-1300 nm (Figure 1.11 and Figure 1.12) of trivalent neptunium ions when compared to previously reported non-aqueous spectra of $NpCl_3(py)_4$ and $NpI_3(THF)_4$.[1.7-1.8] The UV-vis region of all spectra show the color bands of each complex.

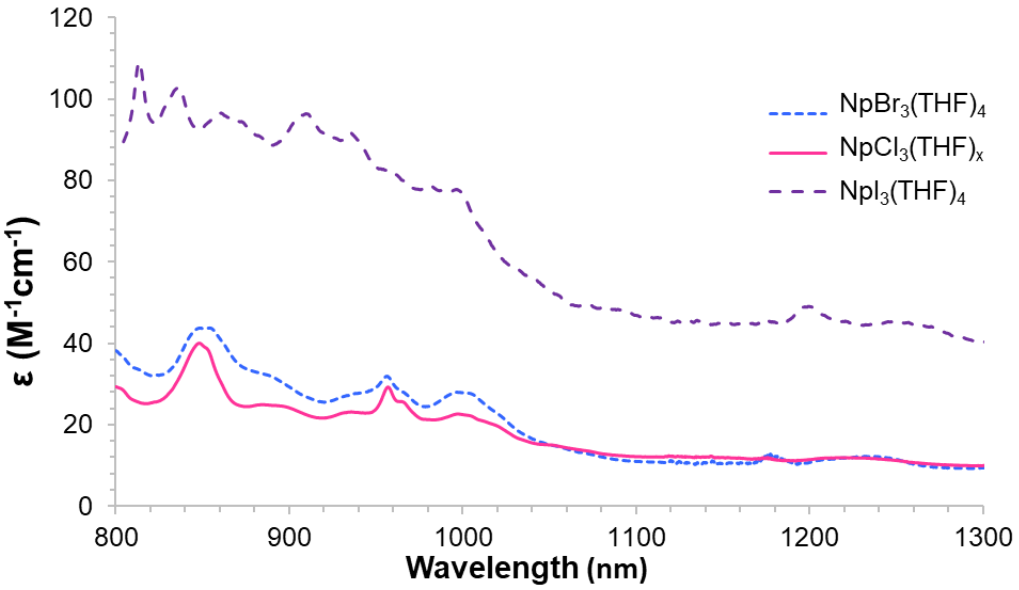

Figure 1.11 NIR at ambient temperature of $NpBr_3(THF)_4$, $NpI_3(THF)_4$, and $NpCl_3(THF)_x$.

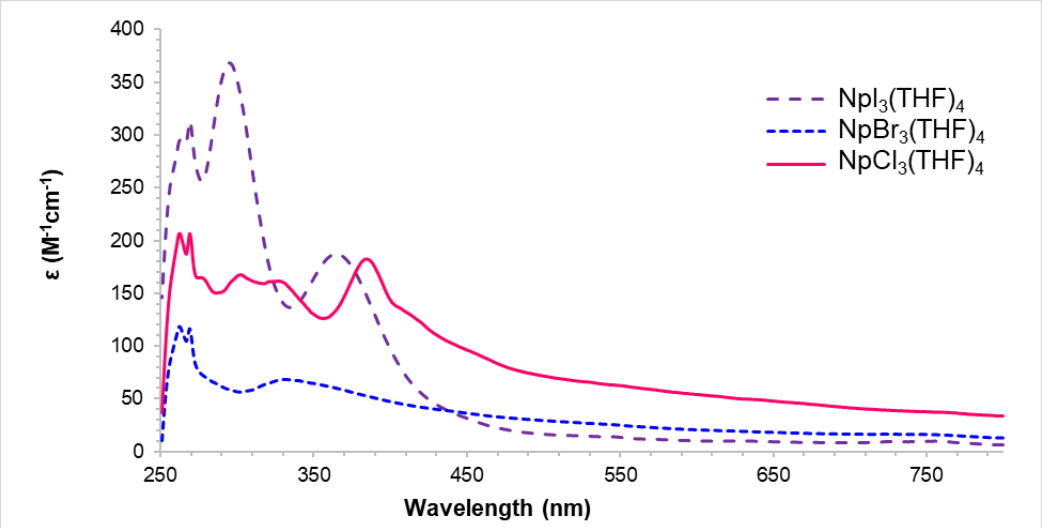

Figure 1.12 UV Vis at ambient temperature of $NpBr_3(THF)_4$, $NpI_3(THF)_4$, and $NpCl_3(THF)_x$.

1.5 Conclusion

In summary, three convenient methods to access trivalent neptunium starting materials without using the metal and elemental halides. The syntheses are clean and yield crystalline material in good yield. These results provide entryway to more convenient trivalent actinide starting materials, specifically trans-uranic elements because the pure metals are rare and not readily available.

1.6 References

1.1) Jones, M. B., & Gaunt, A. J. (2013). Recent Developments in Synthesis and Structural Chemistry of Nonaqueous Actinide Complexes. Chemical Reviews, 113(2), 1137–1198. https://doi.org/10.1021/cr300198m

1.2) Ibers, J. (2010). Neglected neptunium. Nature Chemistry, 2(11), 996–996. https://doi.org/10.1038/nchem.888

1.3) Arnold, P. L., Dutkiewicz, M. S., & Walter, O. (2017). Organometallic Neptunium Chemistry. Chemical Reviews, 117(17), 11460–11475. https://doi.org/10.1021/acs.chemrev.7b00192

1.4) Katz, J. J.; Morss, L. R.; Seaborg, G. T. The Chemistry of the Actinide Elements·, Chapman and Hall: New York, 1986; Vol. 1 and 2 and references therein

1.5) Clark, D. L., Sattelberger, A. P., Bott, S. G., & Vrtis, R. N. (1989). Lewis base adducts of uranium triiodide: A new class of synthetically useful precursors for trivalent uranium chemistry. Inorganic Chemistry, 28(10), 1771–1773. https://doi.org/10.1021/ic00309a004

1.6) Monreal, M. J., Thomson, R. K., Cantat, T., Travia, N. E., Scott, B. L., & Kiplinger, J. L. (2011). UI4(1,4-dioxane)2, [UCl4(1,4-dioxane)]2, and UI3(1,4-dioxane)1.5: Stable and Versatile Starting Materials for Low- and High-Valent Uranium Chemistry. Organometallics, 30(7), 2031–2038. https://doi.org/10.1021/om200093q

1.7) Avens, L. R., Bott, S. G., Clark, D. L., Sattelberger, A. P., Watkin, J. G., & Zwick, B. D. (1994). A Convenient Entry into Trivalent Actinide Chemistry: Synthesis and Characterization of AnI3(THF)4 and An[N(SiMe3)2]3 (An = U, Np, Pu). Inorganic Chemistry, 33(10), 2248–2256. https://doi.org/10.1021/ic00088a030

1.8) Pattenaude, S. A., Anderson, N. H., Bart, S. C., Gaunt, A. J., & Scott, B. L. (2018). Non-aqueous neptunium and plutonium redox behaviour in THF – access to a rare Np(III) synthetic precursor. Chemical Communications, 54(48), 6113–6116. https://doi.org/10.1039/C8CC02611D

1.9) Fetrow, T. V., Grabow, J. P., Leddy, J., & Daly, S. R. (2021). Convenient Syntheses of Trivalent Uranium Halide Starting Materials without Uranium Metal. Inorganic Chemistry. https://doi.org/10.1021/acs.inorgchem.1c00598

1.10) Reilly, S. D., Brown, J. L., Scott, B. L., & Gaunt, A. J. (2013). Synthesis and characterization of NpCl4(DME)2 and PuCl4(DME)2 neutral transuranic An(IV) starting materials. Dalton Transactions, 43(4), 1498–1501. https://doi.org/10.1039/C3DT53058B

1.11) Dutkiewicz, M. S., Farnaby, J. H., Apostolidis, C., Colineau, E., Walter, O., Magnani, N., Gardiner, M. G., Love, J. B., Kaltsoyannis, N., Caciuffo, R., & Arnold, P. L. (2016). Organometallic neptunium(III) complexes. Nature Chemistry, 8(8), 797–802. https://doi.org/10.1038/nchem.2520

1.12) Henrie, D. E., Fellows, R. L., & Choppin, G. R. (1976). Hypersensitivity in the electronic transitions of lanthanide and actinide complexes. Coordination Chemistry Reviews, 18(2), 199–224. https://doi.org/10.1016/S0010-8545(00)82044-5

CHAPTER 2. NEODYMIUM REACTIVITY

2.1 Abstract

Lanthanides are known for maintaining their trivalent oxidation state, meaning they are redox restricted which makes studying multielectron chemistry of interest. Redox chemistry of the redox inactive lanthanide, neodymium was studied using a redox active ligand, $^{Mes}PDI^{Me}$ = 2,6-((Mes)N=CMe)$_2$–C_5H_3N; Mes = 2,4,6-trimethylphenyl. A neodymium dimer with a three minus PDI ligand was used to facilitate multielectron reactivity. The reactivity was explored with multiple oxidants and small molecules to investigate if redox chemistry could be supported by the neodymium complex.

2.2 Introduction

Studying multi electron chemistry with lanthanides is of interest because these metals are known to be redox inactive which makes separations chemistry difficult. Expanding redox chemistry to redox restricted metals is possible with redox active ligands (non-innocent). This chemistry is also of use for modeling reactions for future studies with trans uranic elements such as americium. Previously published series of the neodymium dimer used in these studies were synthesized in a reduction series.[1] The inspiration for studying reactivity with a neodymium metal center comes from two twist boat chalcogenide structures previous reported with a neodymium iminoquinone structure.[2]

2.3 General Considerations

All air- and moisture-sensitive manipulations were performed using standard Schlenk techniques or in an MBraun inert atmosphere drybox with an atmosphere of purified nitrogen.

The MBraun drybox was equipped with a cold well designed for freezing samples in liquid nitrogen as well as two –35 °C freezers for cooling samples and crystallizations. Solvents for sensitive manipulations were dried and deoxygenated using literature procedures with a Seca solvent purification system.1 Benzene-d6 was purchased from Cambridge Isotope Laboratories. Deuterated solvents and degassed by three freeze-pump-thaw cycles and stored over molecular sieves. Benzene-d6 was also stored with sodium metal. $^{Mes}PDI^{Me}$, KC_8, $NdI_3(THF)_{3.5}$, $Nd(^{Mes}PDI^{Me})THF]_2$ were prepared according to literature procedures. [2.1] Neodymium metal was purchased from Strem chemicals. 1H NMR spectra were recorded on a Varian Inova 300 spectrometer at 299.992 MHz. All chemical shifts are reported relative to the peak for $SiMe_4$, using 1H (residual) chemical shifts of the solvent as a secondary standard. The spectra for paramagnetic molecules were obtained by using an acquisition time of 0.5 s; thus the peak widths reported have an error of ±2 Hz. For paramagnetic molecules, the 1H NMR data are reported with the chemical shift, followed by the peak width at half height in Hertz, the integration value, and, where possible, the peak assignment

2.4 Experimental

Reactivity with Benzophenone. In a J-young tube, solid 20 mg of $Nd(PDI)THF]_2$ and solid 11.6 mg of benzophenone were added and dissolved with C_6D_6 and inverted to react.

Reactivity with $(Ph\text{-}S)_2$. In a 20 mL scintillation vial, 50 mg of $Nd(PDI)THF]_2$ was added and dissolved in THF. While stirring, 17.75 mg (2 eq) of $(Ph\text{-}S)_2$ was added slowly. After stirring for one hour the blue solution was filtered over celite then dried to a powder yielding 100 mg. One equivalent of DMAP (7.34 mg) was added to help the material become more crystalline and to solvent swap the bound THF .

Reactivity with (Ph-Te)$_2$. In a J-young tube, solid 20 mg of Nd(PDI)THF]$_2$ and solid 6.55 mg (1 eq) of (Ph-Te)$_2$ were added and dissolved with C_6D_6 and inverted to react.

Reactivity with Se In a J-young tube, solid 20 mg of Nd(PDI)THF]$_2$ and solid 6.32 mg (5 eq) of Se were added and dissolved with C_6D_6 and inverted to react.

Reactivity with Te In a J-young tube, solid 20 mg of Nd(PDI)THF]$_2$ and solid 4.14 mg (2 eq) of Te was added and dissolved with C_6D_6 and inverted to react..

Reactivity with S_8 In a 20 mL scintillation vial, 100 mg of Nd(PDI)THF]$_2$ was added and dissolved in THF. While stirring, 26.14 mg (10/8 eq) S_8 was added slowly. After stirring for one hour the green slurry was filtered over celite then dried to a powder yielding 101 mg.

Reactivity with Azo-mesityl In a J-young tube, solid 50 mg of Nd(PDI)THF]$_2$ and solid 21.28 mg (2 eq) of Azo-Mesityl was added and dissolved with C_6D_6 and inverted to react.

2.5 Results and Discussion

Studies began with synthesis of the neodymium dimer (Nd(^{Mes}PDI^{Me})THF]$_2$ from literature procedures.[2.1] The first reactivity studies were done with benzophenone to break the ketone bond to coordinate oxygen. As seen in figure 2.1, a lot of PDI was displaced into the solution (2.06 ppm, 2.2 ppm, 6.89 ppm, 7.3 ppm and 8.5 ppm) and no neodymium dimer peaks were observed. In figure 2.2, it can be seen that the benzophenone did react since there is no ketone peak (1710 cm^{-1}).

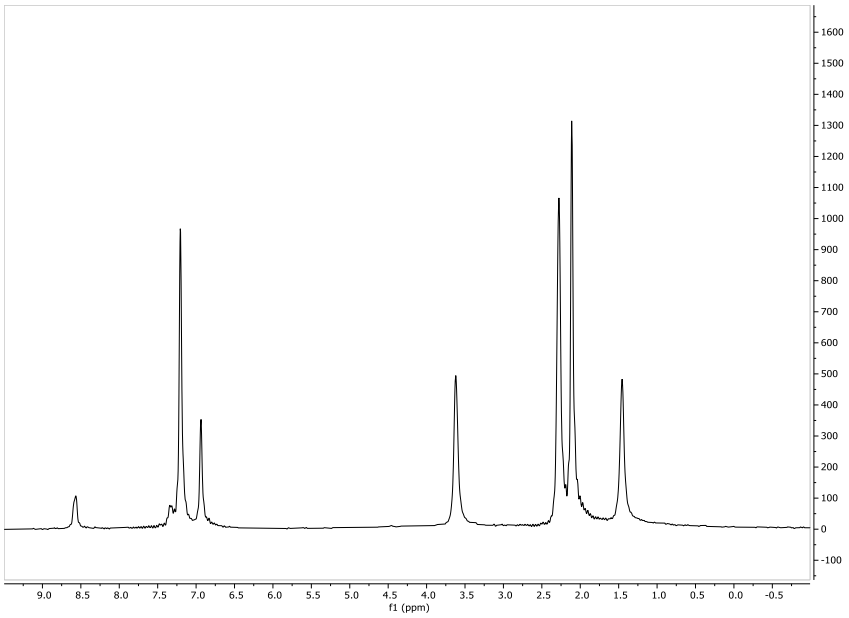

Figure 2.1 1H NMR of benzophenone reactivity.

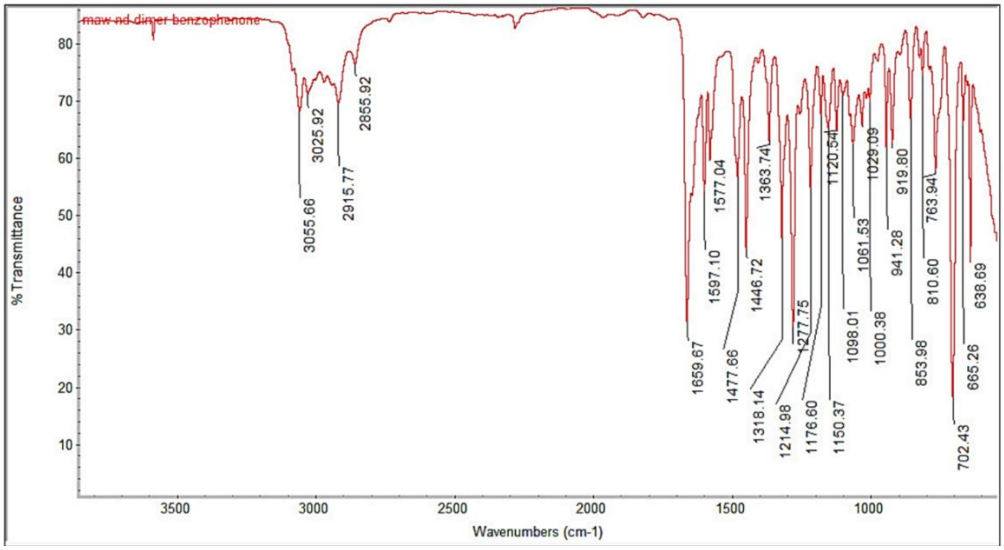

Figure 2.2 IR of benzophenone reactivity solution.

The next exploration of reactivity was performed with chalcogens and chalcogenide derivatives. In figure 2.3 it can be seen that the addition of elemental sulfur results in a displacement of uncoordinated PDI into solution (2.06 ppm, 2.2 ppm, 6.89 ppm, 7.3 ppm and 8.5 ppm) and formation of an unknown product with paramagnetic peaks (1.3 ppm and 3.5 ppm). With the addition of selenium, free PDI is seen in less quantity (figure 2.4) (2.06 ppm, 2.2 ppm, 6.89

ppm, 7.3 ppm and 8.5 ppm) as well as a coordinated THF peaks (1.6 ppm and 3.6 ppm) and unreacted Nd(PDI)THF]$_2$ peaks. The next chalcogen used was tellurium (figure 2.5) which reacted similarly to sulfur, showing displaced free PDI in solution (2.06 ppm, 2.2 ppm, 6.89 ppm, 7.3 ppm and 8.5 ppm), unreacted neodymium dimer (10.5 ppm and 14.23 ppm) forming an unknown product (12.1 ppm and –4.1 ppm).

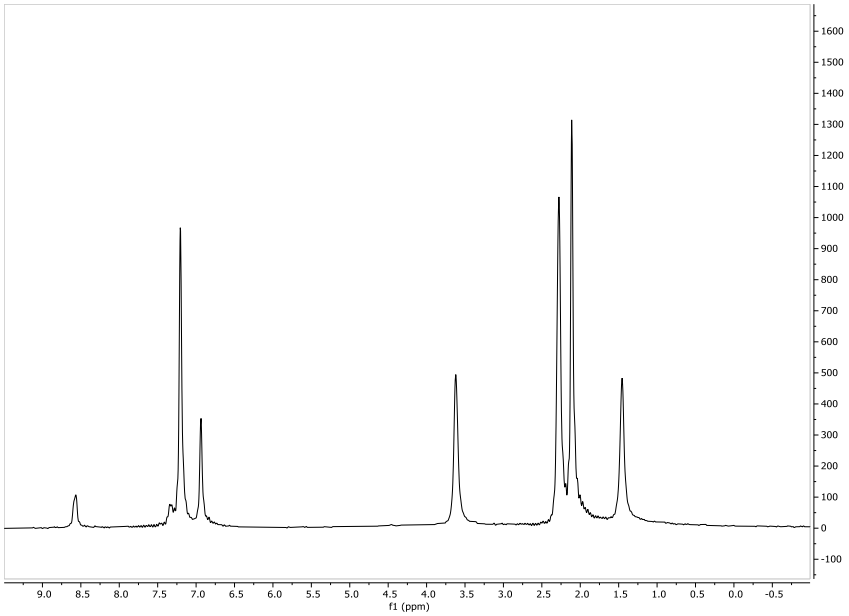

Figure 2.3 1H NMR of sulfur reactivity.

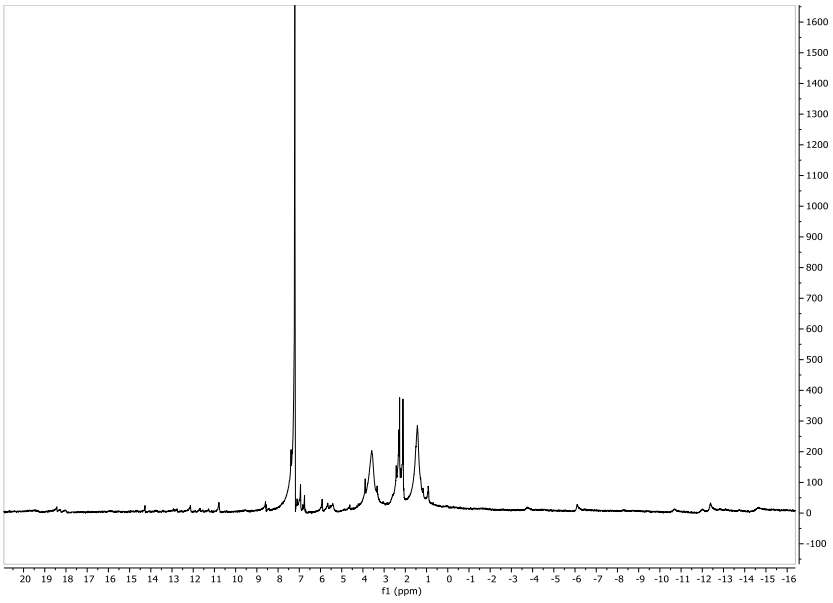

Figure 2.4 ^{1}H NMR of selenium reactivity.

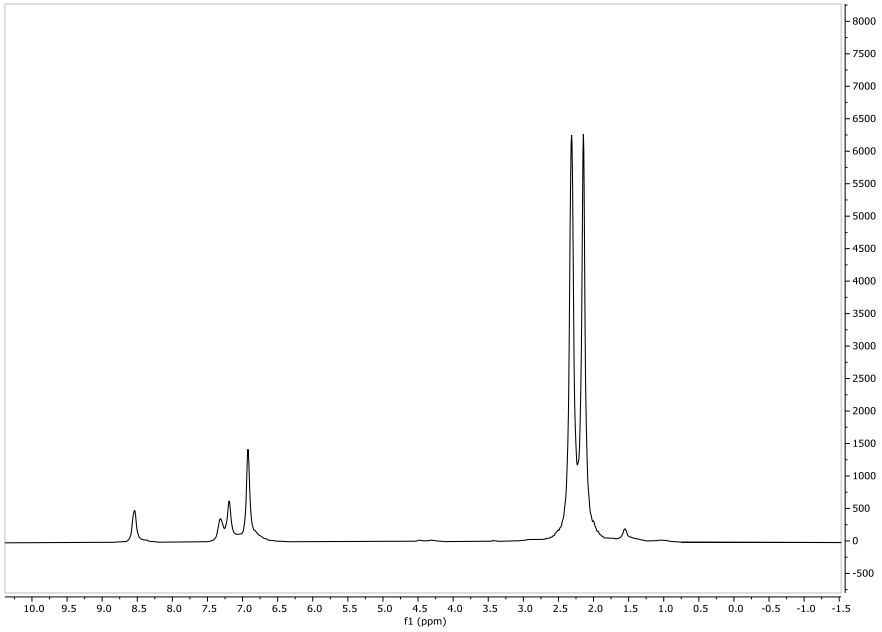

Figure 2.5 ^{1}H NMR of tellurium reactivity.

After the attempts with the elemental chalcogens, the use of substituted chalcogenides were studied. The most promising reactivity is seen in the studies of 5 equivalents of diphenyl-disulfide $(Ph\text{-}S)_2$. There is less PDI that is displaced in solution (2.06 ppm, 2.2 ppm, 6.89 ppm, 7.3 ppm and 8.5 ppm) along with a new set of coordinated THF peaks (3.7 ppm and 1.6 ppm)

and new paramagnetic product peaks (0.89 ppm and 3.0 ppm). To test if the THF was coordinated, DMAP (4-Dimethylaminopyridine) was added to solvent swap the THF molecules (1.5 ppm and 3.5 ppm) coordinated to the neodymium metal center (figure 2.7). The next chalcogen derivative investigated was $(Ph\text{-}Te)_2$ to see if it reacted like the sulfur adduct. The reactivity with one equivalent $(Ph\text{-}Te)_2$ resulted in unreacted neodymium dimer (-17, -6, 0.79, 1.24 ppm, 10.5 ppm, 14.23 ppm and 28.1 ppm) and decomposition of the neodymium dimer (31 ppm) (figure 2.8).

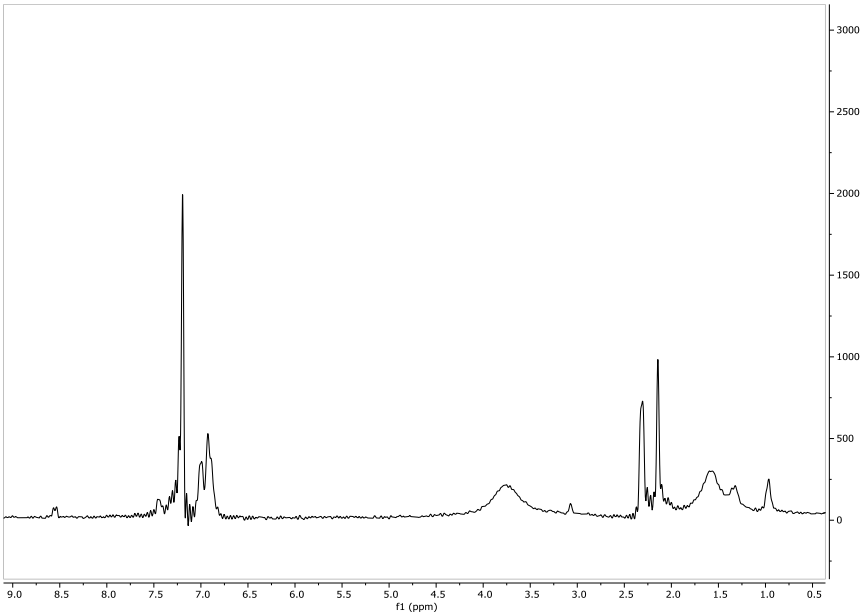

Figure 2.6 1 H NMR of 5 equivalents $(Ph\text{-}S)_2$ reactivity.

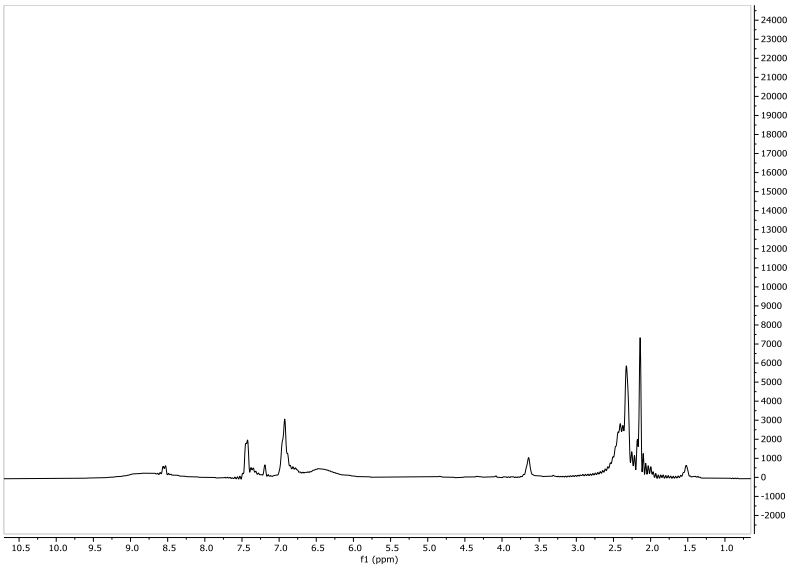

Figure 2.7 1 H NMR of reactivity of $(Ph\text{-}S)_2$ with DMAP.

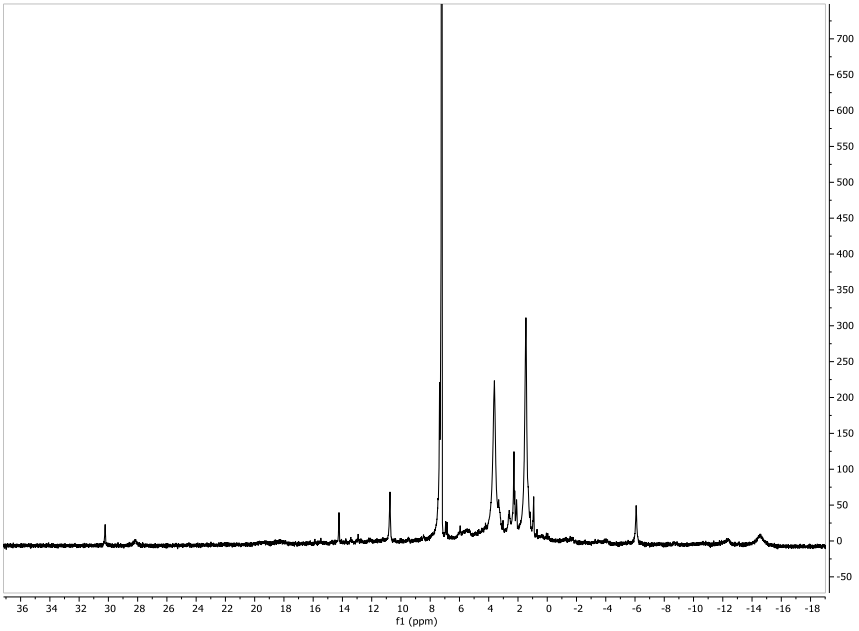

Figure 2.8 1 H NMR of reactivity of 1 equivalent $(Ph\text{-}Te)_2$

Continuing reactivity, azo-mesityl, the methyl substituted version of azobenzene was used to try to break the nitrogen-nitrogen bond and coordinate one nitrogen to the neodymium center. The initial reaction resulted in new paramagnetic peaks and unreacted neodymium dimer

(figure 2.9). After heating the solution overnight at 60 C, new paramagnetic peaks grew in that resembled a new product and peaks from decomposition of the dimer (figure 2.10).

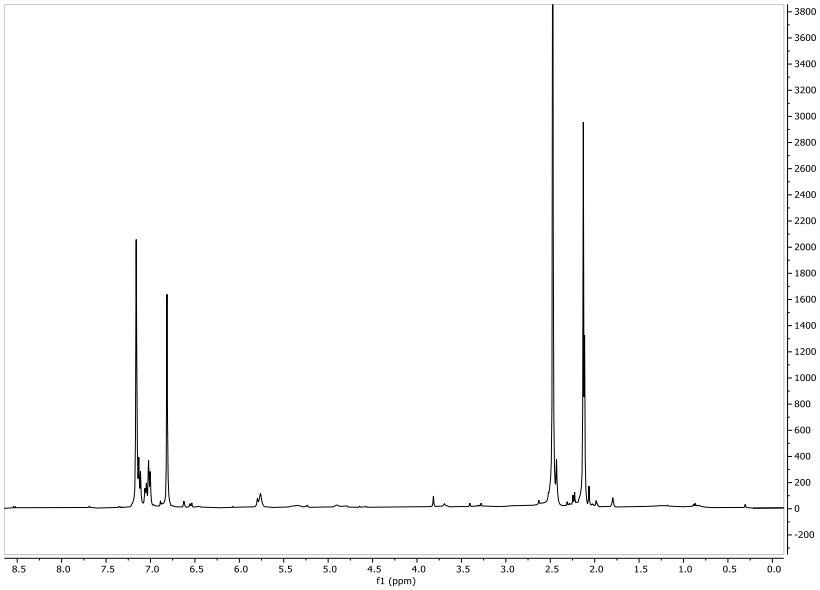

Figure 2.9 1 H NMR of reactivity of Azo-mesityl.

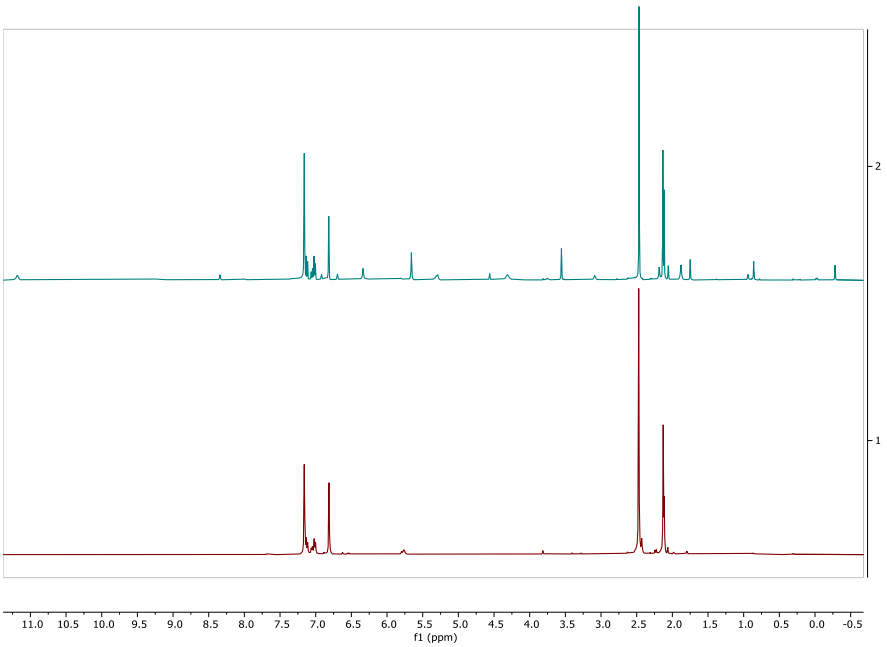

Figure 2.10 Azo Mesityl heated at 60 C overnight (top) versus room temperature reaction.

2.6 Conclusion

In conclusion, a lot of the reactivity in these complexes seem to break the molecule apart and release free PDI into solution with an unknown complex forming. Not knowing the compounds forming is due to difficulties in crystallizing and isolation of clean products, as well as paramagnetic NMR spectra being challenging to assign. There is potential for the $(Ph\text{-}S)_2$ reaction due to it not completely falling apart and seeming to create a 1- PDI ligand radical based on color change and NMR peaks. Reactivity studies continuing for this project could potentially explore another adduct of the pyridine diimine ligand to see if this aids in crystallizations, such as replacing the mesityl with a dipp group (2,6-diisopropylphenyl). Another idea would be to use non-paramagnetic lanthanides such as lanthanum for more straightforward NMR assignment. Additionally, using samarium would be an interesting series to investigate due to the metal being able to be stable in a divalent state, allowing more multielectron chemistry. It would be interesting to see if samarium would reduce to the divalent oxidation before the PDI ligand reducing, or if the PDI can be fully reduced as well as the samarium being divalent.

2.7 References

2.1) Galley, S. S., Pattenaude, S. A., Higgins, R. F., Tatebe, C. J., Stanley, D. A., Fanwick, P. E., Zeller, M., Schelter, E. J., & Bart, S. C. (2019). A reduction series of neodymium supported by pyridine(diimine) ligands. Dalton Transactions, 48(23), 8021–8025. https://doi.org/10.1039/C9DT00679F

2.2) Coughlin, E. J., Zeller, M., & Bart, S. C. (2017). Neodymium(III) Complexes Capable of Multi-Electron Redox Chemistry. Angewandte Chemie International Edition, 56(40), 12142–12145. https://doi.org/10.1002/anie.201705423

LIST OF PUBLICATIONS

1. **Whitefoot, M.A**.; Perales, D.; Zeller, M.; Bart, S.C.; "Synthesis of Non-aqueous Neptunium (III) Halide Solvates from Neptunia." *Angew. Chem.* **2021 Submitted.**

2. Galley, S. S.; Pattenaude, S. A.; Ray, D.; Gaggoli, C.; **Whitefoot, M. A.;** Qiao, Y.; Nelson, W. L.; Baumbach, R.; Sperling, J. M.; Zeller, M.; Collins, T. S.; Schelter, E. J.; Gagliardi, L; Albrecht-Schönzart, T. E; Bart, S. C; "Using Redox-Active Ligands to Generate Actinide Ligand Radical Species" *Inorg. Chem.* **2021 Submitted.**

3. Sperling, J. M.; Warzecha, E.; Klamm, B. E.; Gaiser, A. N.; Windorff, C. J.; **Whitefoot, M. A.;** Albrecht-Schönzart, T. E.; "Pronounced Pressure Dependence of Electronic Transitions for Americium Compared to Isomorphous Neodymium and Samarium Mellitates" *Inorg. Chem.* **2021**, 60, 1, 476-483. DOI: 10.1021/acs.inorgchem.0c03293

4. Sperling, J. M.; Warzecha, E.; Celis-Barros, C.; Sergentu, D. C.; Wang, X.; Klamm, B. E.; Windorff, C. J.; Gaiser, A. N.; White, F. D.; Beery, D. A.; Chemey, A. T.; **Whitefoot, M. A.;** Long, B. N.; Hanson, K.; Zurek, E.; Autschbach, J.; Albrecht-Schönzart, T. E.; "Compression of Curium Pyrrolidinedithiocarbamate Enhances Covalency" *Nature,* **2020,** 583, 396-699. DOI: 10.1038/s41586-020-2479-2

5. Sperling, J. M.; Warzecha, E.; Windorff, C. F.; Klamm, B. E.; Gaiser, A. N.; **Whitefoot, M. A.;** White, F. D.; Poe, T. N.; Albrecht-Schönzart, T. E.; "Pressure-Induced Spectroscopic Changes in a Californium 1D Material are Twice as Large as Found in the Holmium Analog" *Inorg. Chem.* **2020,** 59, 15, 10794-10801. DOI: 10.1021/acs.inorgchem.0c01290

6. Sperling, J. M.; Gaiser, A. N.; Windorff, C. J.; Klamm, B. E.; **Whitefoot, M. A**.; Chemey, A. T.; Long, B. N.; Campbell, J. G.; Albrecht-Schmitt, T. E.; "Structural and Spectroscopic Investigation of Two Plutonium Mellitates" *Inorg. Chem.* **2020,** 59, 5, 3085-3090. DOI: 10.1021/acs.inorgchem.9b03432